Practical Model to Estimate Behavior of Tsunami-Drifted Bodies

by

Takashi Tomita[1] and Kazuhiko Honda[2]

ABSTRACT

Historical records of tsunami damage have shown us that tsunamis cause various damages: inundation, destruction of houses, drift of vessels and others. If vessels are drifted by a tsunami, they have the potential to collide with houses and buildings and then to cause secondary damage to them in addition to the damage by tsunami fluid force. To control and mitigate the damages by the drifted-bodies, we should understand and predict the damages at first. We have, therefore, developed a numerical model to estimate behavior of multiple tsunami-drifted bodies practically. The present model calculates drift motion of each body in terms of drag and inertia forces acting on the body, and furthermore considers collision between drifted bodies and between the drifted body and any structure. After the present model is implemented into the STOC system which calculates tsunami damages in oceans and coastal areas, it is validated qualitatively in comparison with some simple test runs and applied to the calculation in a model area with actual bathymetry and topography.

KEYWORDS: Collision, Drifted Body, Numerical Modeling, Tsunami

1. INTRODUCTION

Japan has good system to issue tsunami warning. The Japan Meteorological Agency (JMA) is the organization in charge. Local governments also issue evacuation order and advisory if happen of tsunami damage is estimated in their regions. However, even if the tsunami warning and evacuation order are issued, many residents stay at their houses and offices to get further information of tsunami and do not evacuate actually. Is this good behavior? Each person decides finally whether he/she should evacuate or not. Therefore, it is important that each person images tsunami disasters which he/she may suffer, before encounter of the tsunami.

To help the enhancement of people's imagination of tsunami disasters, we have developed numerical simulation and visualization system on tsunami damage, which is named the STOC system [1]. As introduced in the 40th panel meeting in the NIST, the STOC system consists of the numerical simulation model named STOC (Storm surge and Tsunami simulator in Oceans and Coastal areas) and a display tool which shows easily numerical results such as the variation of water surface elevation and water particle velocity as well as damage occurrence areas by using the moving images. Another feature of the display tool is that users of the tool can see the results from any viewpoint they want.

As shown in historical damage records, tsunamis cause inundation, destruction of houses as well as drift of many vessels and others. If vessels are drifted by a tsunami, they may collide with houses and buildings, and then cause secondary damage to them in addition to the damage by tsunami fluid force. To control and mitigate damages by the drifted bodies, we should understand and estimate their behavior. A new numerical model is, therefore, developed and implemented in the STOC system to estimate the behavior of tsunami-drifted bodies. The attractive features of the model are as follows: 1) it can deal with a large number of bodies, 2) calculate not only translational motion of each body but rotational motion in the horizontal plane, and 3) consider collision between the drifted bodies and between the body and any structure

1 Research Director, Tsunami Research Center, Port and Airport Research Institute, 3-1-1 Nagase Yokosuka 239-0826, Japan
2 Researcher, ditto.

2. NUMERICAL SIMULATOR OF STOC FOR ESTIMATION OF TSUNAMI DAMAGE

The STOC system is composed of two parts: numerical simulation model and display toll of its results. The simulation model also consists of 3 sub-models: STOC-ML, STOC-IC and STOC-DM. Figure 1 shows an example of arrangement of STOC-ML, STOC-IC and STOC-DM.

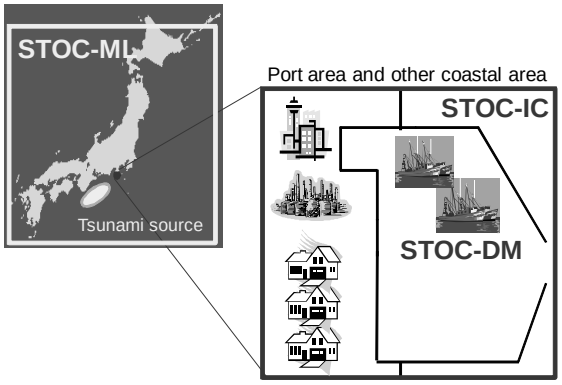

Fig. 1 Arrangement of STOC-ML, STOC-IC and STOC-DM in the numerical simulation model of the STOC system

STOC-ML [1] is a multi-level model which is developed with the use of hydrostatic pressure assumption, and therefore can be applied in wide area such as oceans. To consider vertical distribution of horizontal velocity, STOC-ML deals with a water basin vertically divided into some layer. STOC-IC [1] is the fully three-dimensional model, whose governing equations are the continuity equation to express the mass conservation and the Reynolds-Averaged Navier-Stokes (RANS) equations as the momentum equations in three dimensions. The porous body model by Sakakiyama and Kajima [2] is introduced in the discretized equations of the governing equations to consider the configuration of sea bottom and the shape of structures smoothly. The eddy viscosity is also considered in terms of implementation of the eddy viscosity coefficient which depends on velocity structure and a model coefficient in the same way as Fujima et al. [3]. Comparison with the hydraulic experiment, in which tsunami reduction was investigated around a tsunami breakwater, showed that the tsunami was not sensitive to the model coefficient in the eddy viscosity coefficient [4]. Therefore, we may use the default value of the coefficient.

STOC-DM is the new model added into the STOC system to calculate the tsunami-drifted vessels, cars, containers and other. To calculate behavior of the tsunami-drift bodies, this model uses temporal and special variation data of water surface elevation and horizontal velocity calculated by STOC-ML and STOC-IC. The details of the model are in the next section.

Easy showing of numerical simulation results is important for residents who may not necessarily have enough knowledge to see the results. For

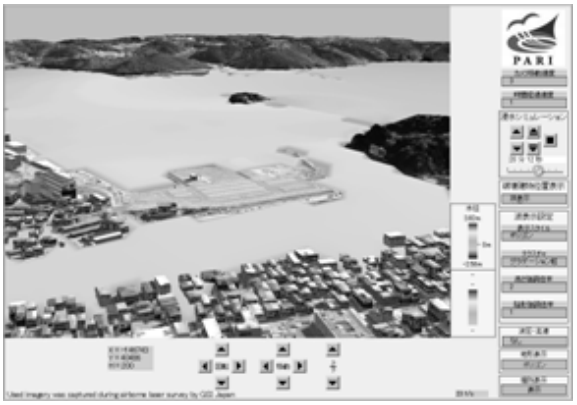

Fig. 2 Snapshot of display on water surface elevation using the STOC system

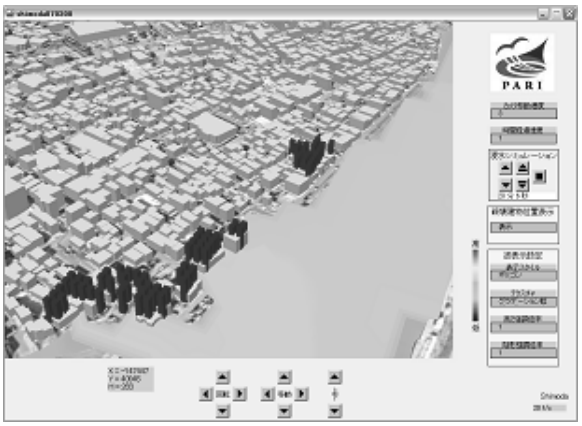

Fig. 3 Snapshot of display on damage occurrence areas using the STOC system (Black bars indicate damage occurrence areas)

example, a resident may want to see the result of tsunami damage estimation in the whole area of their city as well as in his/her residential area. To satisfy such a demand of each resident and disaster mitigation officer, the display tool of the STOC system has the function of showing the results from any viewpoints. Furthermore, the displayed results are not only inundation area and its depth but fluid velocity and wave pressure, which are calculated by the STOC system. Figures 2 and 3 show examples of tsunami inundation and tsunami-damaged areas indicated by the display tool. Actually the tool shows the results by the moving images, although the figures indicate snapshots.

3. NUMERICAL MODEL TO ESTIMATE DRIFT MOTION OF BODIES BY TSUNAMIS

3.1 Drift Motion Model

To calculate drift motion of many bodies by a series of tsunami waves with less computational efforts, the numerical model to solve drift motion of bodies does not calculate water surface elevation and water particle velocity of tsunami directly, and utilizes the results on them which are calculated by the other numerical models of tsunami. Then, each body is horizontally moved by the tsunami-induced drag and inertia forces acting on each body.

For practical calculation, the shape of each drifted body is approximated by a rectangular solid. Three modes of motion are calculated in the model: surging, swaying and yawing, as shown in Fig. 4. It should be noted that the vertical motion of heaving is considered so as to keep draft of the body on the water surface. Therefore, the vertical motion is induced by the buoyancy force of the body.

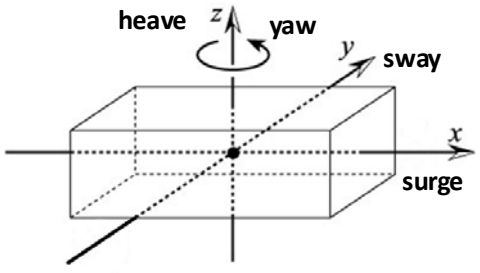

Fig. 4 Considered motion of drifted body

With reference to Ikeya et al. [5], horizontal forces in the surging and swaying directions, F_x and F_y, respectively, and momentum around the z-direction, M_z, are determined by the following equations:

$$\left.\begin{aligned} F_X &= (1-\omega)F_{DX1} + \omega F_{DX2} + F_{MX} \\ F_Y &= (1-\omega)F_{DY1} + \omega F_{DY2} + F_{MY} \\ M_Z &= (1-\omega)M_{DZ1} + \omega M_{DZ2} + M_{MZ} \end{aligned}\right\} \quad (1)$$

in which

$$\omega = \begin{cases} 1.0 - \dfrac{0.95}{0.2}\left(\dfrac{h}{D} - 1.0\right): & 1 < \dfrac{h}{D} \le 1.2 \\ 0.05: & 1.2 < \dfrac{h}{D} \end{cases} \quad (2)$$

$$\left.\begin{aligned} F_{DX1} &= +\frac{\rho}{2}\iint_{sm} C_{DX1,sm} U_{sm} |U_{sm}| dYdZ \\ &\quad +\frac{\rho}{2}\iint_{sn} C_{DX1,sn} U_{sn} |U_{sn}| dYdZ \\ F_{DY1} &= +\frac{\rho}{2}\iint_{ps} C_{DY1,ps} V_{ps} |V_{ps}| dXdZ \\ &\quad +\frac{\rho}{2}\iint_{sb} C_{DY1,sb} V_{sb} |V_{sb}| dXdZ \\ M_{DZ1} &= -\frac{\rho}{2}\iint_{sm} C_{DX1,sm} U_{sm} |U_{sm}| YdYdZ \\ &\quad -\frac{\rho}{2}\iint_{sn} C_{DX1,sn} U_{sn} |U_{sn}| YdYdZ \\ &\quad +\frac{\rho}{2}\iint_{ps} C_{DY1,ps} V_{ps} |V_{ps}| XdXdZ \\ &\quad +\frac{\rho}{2}\iint_{sb} C_{DY1,sb} V_{sb} |V_{sb}| XdXdZ \end{aligned}\right\} \quad (3)$$

$$\left.\begin{aligned} F_{DX2} &= \frac{\rho}{2} C_{DX2}\left(U_G^2 + V_G^2\right)\frac{U_G}{|U_G|} BD \\ F_{DY2} &= \frac{\rho}{2} C_{DY2}\left(U_G^2 + V_G^2\right)\frac{V_G}{|V_G|} LD \\ M_{DZ2} &= l\sqrt{F_{DX2}^2 + F_{DY2}^2} \end{aligned}\right\} \quad (4)$$

$$\left.\begin{aligned} F_{MX} &= \frac{\rho}{2} C_M LD\left(\int_{sm}\frac{\partial U_{sm}}{\partial t}dY + \int_{sn}\frac{\partial U_{sn}}{\partial t}dY\right) \\ F_{MY} &= \frac{\rho}{2} C_M BD\left(\int_{ps}\frac{\partial V_{ps}}{\partial t}dX + \int_{sb}\frac{\partial V_{sb}}{\partial t}dX\right) \\ M_{MZ} &= -\frac{\rho}{2} C_M LD\left(\int_{sm} Y\frac{\partial U_{sm}}{\partial t}dY + \int_{sn} Y\frac{\partial U_{sn}}{\partial t}dY\right) \\ &\quad +\frac{\rho}{2} C_M BD\left(\int_{ps} X\frac{\partial V_{ps}}{\partial t}dX + \int_{sb} X\frac{\partial V_{sb}}{\partial t}dX\right) \end{aligned}\right\} \quad (5)$$

L, B and D are the length, width and draft depth of floating body, and h the water depth, as shown in Fig. 5. In Eq. 3, U_{sm}, U_{sn}, V_{ps} and V_{sb} are the distributed flow velocities on the side faces of body, as shown in Fig. 6. It is necessary that these velocities should be calculated in the situation of no drifted body. In Eq. 4, U_G and V_G are the flow velocities in the surging and swaying directions at the position of the center of gravity of the body as shown in Fig. 6. The first and second terms in the right-hand side of Eq. 1 mean drag forces induced by the flows going under the bottom of body and running through the sides, respectively. The third terms are for inertia force. In the calculation of F_{DX1}, F_{DY1} and M_{DZ1}, velocity distribution in the horizontal plane is considered, because eddies shedding from the bottom may not be uniform horizontally depending on the non-uniform velocity. It should be noted that M_{DZ1} is modified because a drifted body with rotational motion and the same drift speed as the surrounding flow makes rotations indefinitely using the original M_{DZ1} by Ikeya et al.

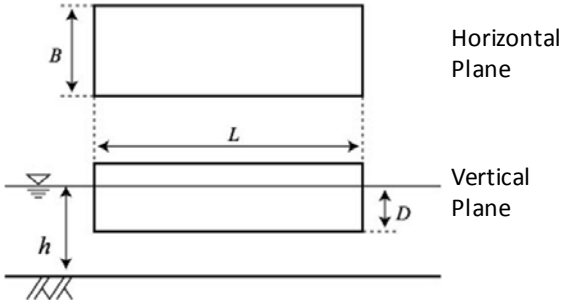

Fig. 5 Definition of size of body

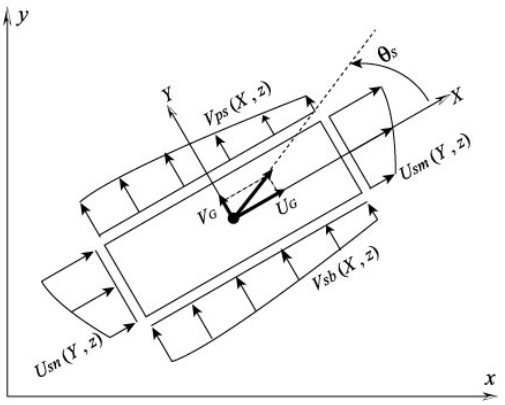

Fig. 6 Definition of flow velocities to calculate fluid forces

The coefficients such as $C_{DX1,sm}$ and others are as follows:

$$\left.\begin{aligned} C_{DX1,sm} &= \begin{cases} 0.4 & : U_{sm} \geq 0 \\ 0.8 & : U_{sm} < 0 \end{cases} \\ C_{DX1,sn} &= \begin{cases} 0.8 & : U_{sn} \geq 0 \\ 0.4 & : U_{sn} < 0 \end{cases} \\ C_{DY1,ps} &= \begin{cases} 0.4 & : V_{ps} \geq 0 \\ 0.8 & : V_{ps} < 0 \end{cases} \\ C_{DY1,sb} &= \begin{cases} 0.8 & : V_{sb} \geq 0 \\ 0.4 & : V_{sb} < 0 \end{cases} \end{aligned}\right\} \quad (6)$$

$$\left.\begin{aligned} C_{CX2} &= 2.0\left(\cos^2\theta_s + 1.2\left|\sin\theta_s \cos\theta_s\right|\right) \\ C_{CY2} &= 2.0\left(\sin^2\theta_s + 2.2\left|\sin\theta_s \cos\theta_s\right|\right) \end{aligned}\right\} \quad (7)$$

$$C_M = 2.0 \quad (8)$$

$$l = \begin{cases} +0.09L\left|\sin(2\theta_s)\right|^{1.2} : \sin(2\theta_s) \geq 0 \\ -0.09L\left|\sin(2\theta_s)\right|^{1.2} : \sin(2\theta_s) < 0 \end{cases} \quad (9)$$

3.2 Collision Model

For easily searching a contact point of a drifted body to another body or a structure, it is assumed that a contact face is set so as to cover all main parts of the body, as shown in Fig. 7, which shows an example of a fishing boat. The horizontal shape of a ship which is inscribed in the rectangular indicated by the actual body length of L_C and actual body width of B_C is surrounded by a contact face line with circular curves with the radius of R_C (m) and parallel lines with the spacing of $2R_C$ (m). The vertical section of contact face is the rectangular to covers main parts which may collide with anybody. It should be noted that the volume formed by the contact face is different from the volume for calculation of drift motion, which is indicated in terms of L, B and H in Fig. 5. The values of L and B are determined by Eq. 10, considering Eq. 11. Eq. 10 expresses the balance of mass and buoyancy of the body, in which M is the mass of body, D the draft depth of body and ρ_w the density of water. In deed

$$M = \rho_w LBH \quad (10)$$

$$\left.\begin{aligned} L &\leq L_C \\ B &\leq B_C \\ H &\geq D \end{aligned}\right\} \quad (11)$$

At the moment that the drift body collides with anything, it is assumed that the moving speed of the drift body suddenly becomes zero in the normal direction of the contact face without deformation.

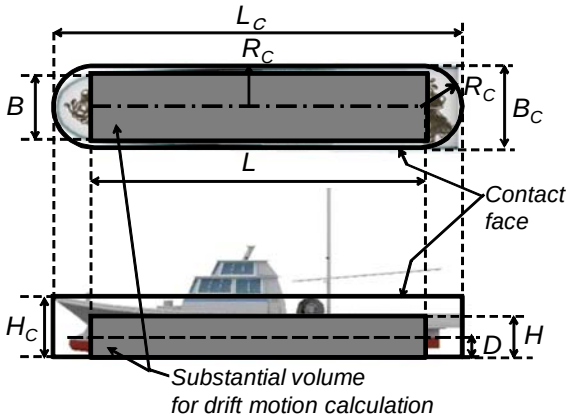

Fig. 7 Contact face and substantial volume of mass to calculate drift motion

4. TEST CALCULATIONS IN SIMPLE CONDITIONS

Validation of the drift model is conducted under very simple calculation conditions. In the phase 1 of test runs, drift motion of a floating body in a uniform flow has been investigated, in which the initial body's angle in the flow, the partition number of the body to consider the velocity distribution in space, and ratio of water depth and draft depth have been changed. The number of test runs is eight. In the phase 2, a moving body contacting with a structure and two bodies colliding with each other have been checked. The number of test runs is seven. In total 15 runs, the developed drift model provided good results qualitatively.

Figure 8 show a result of the test calculation in the phase 2, in which a floating body is initially set in the flow of u= 0.5 m/s in the x-direction and v = 0.5 m/s in the y-direction. The body scales are 3 m in the x-direction, 15 m in the y-direction, and 1 m of draft depth, the mass of body is 45 t. In the figure, locations of the drifted body are indicated every 30 s. Before colliding with the structure, the angle of body gradually turned to the flow direction as it is drifted by the uniform flow, and the moving speed of the body is also accelerated. After colliding with a corner of structure, the body rotates in anti-clockwise direction around the corner, and the body collides again with the side of structure. Figures 9 and 10 show the motion velocity of the drifted body and rotation angle, respectively. Until 350 s when the drifted body contacts the structure first, the direction of body changes toward 45° which is the flow direction, the motion speed is also accelerated toward the flow velocity. After colliding, the motion speed is suddenly down.

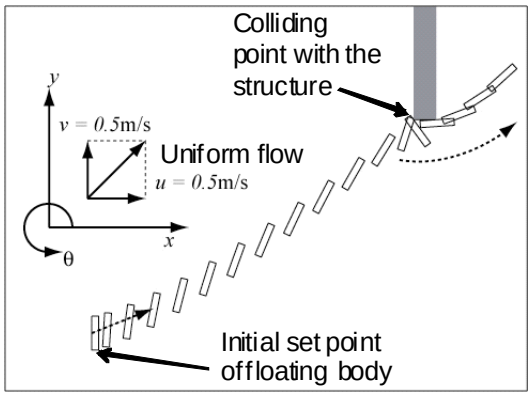

Fig. 8 Motion of the drifted body in a uniform flow (Case 1-1)

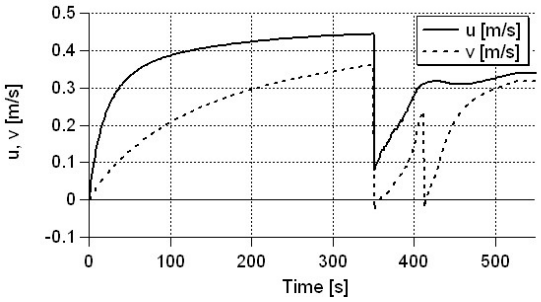

Fig. 9 Motion speed of the drifted body

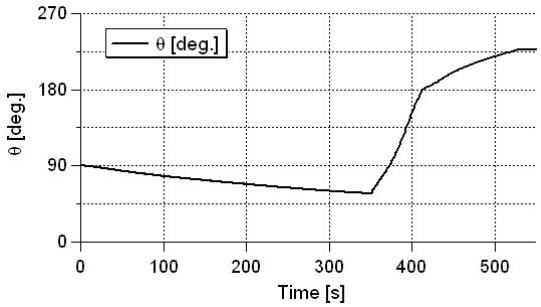

Fig. 10 Direction angle of the drifted body

5. APPLICATION OF STOC SYSTEM INCLUDING WITH DRIFT MODEL TO ACTUAL BATHYMETRY AND TOPOGRAPHY

The STOC system is applied to a model area with actual bathymetry and topography, as shown in Fig. 11. Many fishing boats are moored in the water area covered by the dashed thin line, as shown in Picture 1. Since air-born laser profiler data is available in the model area, we can use the calculation grid size of 2 m in the area surrounded by the dashed thick line in the figure where STOC-IC is applied to calculate the tsunami in detail. In the outer region, STOC-ML with a single layer is applied, and the grid size of 6 m is especially used in the area indicated in the figure. STOC-ML and STOC-IC is connected to conduct sequence of tsunami calculation.

The generated tsunami in the calculation has the tsunami height of 2 m approximately and wave period of 20 minutes at Point A in Fig. 11 in the situation of no breakwaters. If there are the breakwaters as shown in the figure, the tsunami does not overtop them, and they can reduce the tsunami intrusion into the harbor area. If a submerged breakwater is additionally installed in the opening section of the breakwaters, it is anticipated to reduce further the tsunami height in the harbor area. As a trial to check the performance of the STOC system, tsunami calculation by the STOC system is conducted in the situation of existence of the breakwaters with the submerged breakwater, because experimental validation of the STOC system has shown that it can solve the tsunami passing through breakwaters with the submerged breakwater [4, 5]. The calculation conditions are as follows: in Case 1 no breakwaters are installed, and in Case 2 there are breakwaters with the submerged breakwater which narrow their opening section area from 27,000 m^2 to 1,800 m^2. The number of moored vessels is 158 in the harbor area. In this trial, only the first tsunami is picked up in a series of tsunami waves. The initial water surface level is 0.7 m above the mean water level.

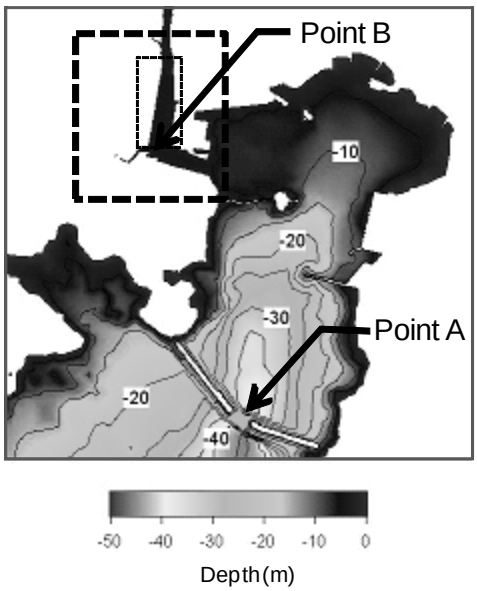

Fig. 11 Model area where the STOC system is applied

Picture 1 Moored vessels in the model area

Figure 12 shows variations of water surface elevation at Point A and Point B. The water surface elevation at Point B rises 3.2 m from the initial water surface level (3.9 m from the mean water level) in the case of no breakwaters. However, in the situation of existence of the breakwaters, it decreases to 2.2 m (2.9 m). Since the ground height is approximately 0.8 m above the initial water level (1.5 m above the mean water level) around Point B, the tsunami runs up on the land even if the breakwaters are installed. However, inundation depth is less than 2 m, and then may not cause severe destruction of houses by the tsunami. Indeed, Shuto [6] and damage reports on the 2004 Indian Ocean Tsunami have indicated that the tsunami of 2 m or more provides complete destruction of wooden houses.

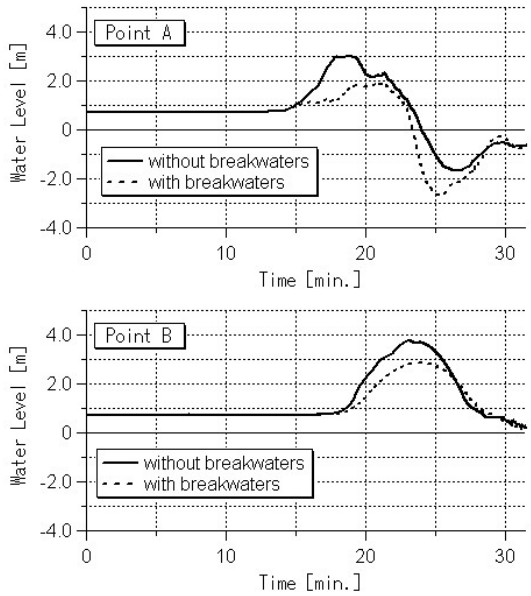

Fig. 12 Time variations of water surface elevation

The fluid velocity is also reduced from 3.5 m/s to 2.1 m/s, as shown in Fig. 13 by the installation of the breakwaters. However, it should be noted that at the opening section of breakwaters (at Point A) the fluid velocity is fastened depending on narrowing of the opening section. Therefore, we should consider such a fast fluid velocity for design of the breakwater.

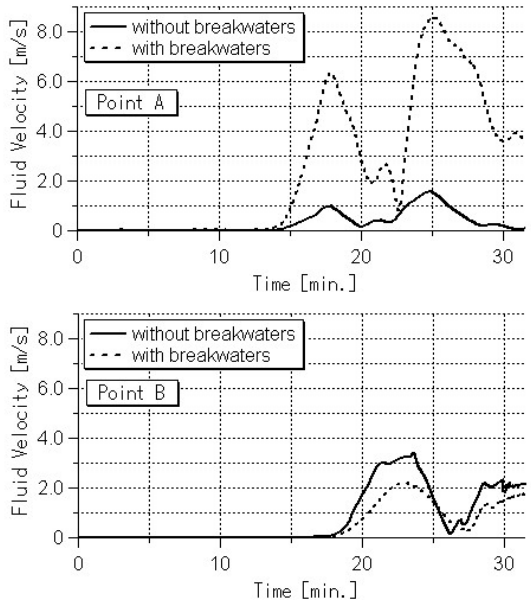

Fig. 13 Time variations of fluid velocity

The breakwaters have another function to control tsunami damage. In this trial, they delay the start of tsunami inundation 90 seconds in residential area near the coast line. This time duration provides evacuating people with advantages.

The reduction of water surface elevation and fluid velocity also provides reduction of the number of drifted vessels. Figure 14 shows the situations just before inundation starts and 3 minutes after the start of inundation. Both of them are of the case of no breakwaters. In the case of no breakwaters, the tsunami with high water surface elevation and fast fluid velocity drifts 56 vessels: 49 vessels broken the mooring system, and 7 vessels settled on the land. All boats are not necessarily swept by the tsunami in the case of no breakwaters. However, if the breakwater is installed, the first tsunami wave sweeps only 7 vessels on the land.

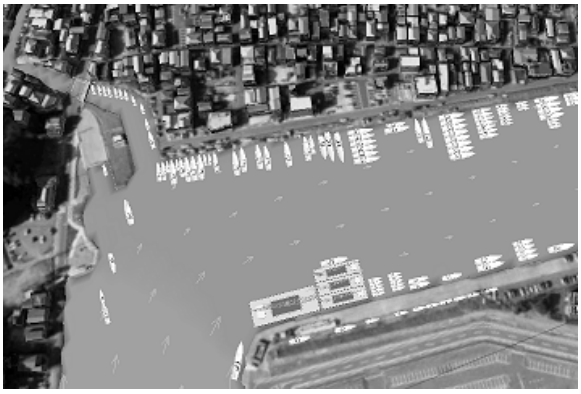

(1) Just before inundation starts

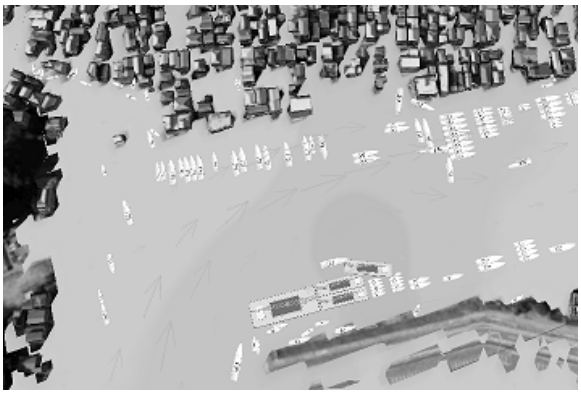

(2) 3.6 minutes after the start of inundation

Fig. 14 Snapshots of drifted vessels in the case of no breakwaters, using STOC's display tool

6. CONCLUDING REMARKS

The new numerical model is implemented in the STOC system to calculate the drift behavior of vessels and others by tsunamis. The model can deal with their collision with structures and another drifted body.

Validation of the model is conducted in the very simple test runs, and it is confirmed that the model gives us good results. Furthermore, we need to validate the model quantitatively.

As a trial to show how damage estimation we do by the STOC system including the drift model, the system is applied to a model area with actual bathymetry and topography. Existence of breakwaters, on which the STOC system is already validated in comparison with experimental results quantitatively, reduces inundation depth, fluid velocity in the harbor area and the number of drifted vessels, and delays the start of inundation.

ACKNOWLEDGEMENT

We express sincere thanks to the Geographical Survey Institute Japan for supplying the airborne laser scanning survey data of the model area.

REFERENCES

1. Tomita, T., K. Honda, and T. Kakinuma. 2007. Application of three-dimensional tsunami simulator to estimation of tsunami behavior around structures. *Proceedings of the 30th International Conference on Coastal Engineering*, ASCE, 1677-1688.
2. Sakakiyama, T., and R. Kajma. 1992. Numerical simulation of nonlinear wave interacting with permeable breakwater, *Proceedings of 23rd International Conference on coastal Engineering*, ASCE, 1517-1530.
3. Fujima, K., K. Masamura, and C. Goto. 2002. Development of the 2d/3d hybrid model for tsunami numerical simulation, *Coastal Engineering Journal*, JSCE, 44(4), 373-397.
4. Tomita, T. and K. Honda. 2009. Tsunami inundation simulation by three-dimensional model, Proceedings of *the 31st International Conference on Coastal Engineering*, ASCE (in press).
5. Ikeya, T., R. Asakura, N. Fujii, M. Ohmori, T. Takeda and K. Yanagisawa. 2005. Experiment on tsunami wave force acting on a floating body and development of an evaluation method, *Proceedings of Annual Journal of Coastal Engineering*, JSCE, 52, 761-765 (in Japanese).
6. Shuto N. 1993. Tsunami intensity and disasters. *In Tsunamis in the world, edited by Tinti, S.*, Kluwer Academic Press, 197-216.